

Fully Kinetic Simulations of Dense Plasma Focus Z-Pinch Devices

A. Schmidt,¹ V. Tang,¹ and D. Welch²

¹Lawrence Livermore National Laboratory, 7000 East Avenue, L-227 Livermore, California 94550, USA

²Voss Scientific, 418 Washington Street Southeast, Albuquerque, New Mexico 87108, USA

(Received 16 July 2012; published 14 November 2012)

Dense plasma focus Z-pinch devices are sources of copious high energy electrons and ions, x rays, and neutrons. The mechanisms through which these physically simple devices generate such high-energy beams in a relatively short distance are not fully understood. We now have, for the first time, demonstrated a capability to model these plasmas fully kinetically, allowing us to simulate the pinch process at the particle scale. We present here the results of the initial kinetic simulations, which reproduce experimental neutron yields ($\sim 10^7$) and high-energy (MeV) beams for the first time. We compare our fluid, hybrid (kinetic ions and fluid electrons), and fully kinetic simulations. Fluid simulations predict no neutrons and do not allow for nonthermal ions, while hybrid simulations underpredict neutron yield by $\sim 100\times$ and exhibit an ion tail that does not exceed 200 keV. Only fully kinetic simulations predict MeV-energy ions and experimental neutron yields. A frequency analysis in a fully kinetic simulation shows plasma fluctuations near the lower hybrid frequency, possibly implicating lower hybrid drift instability as a contributor to anomalous resistivity in the plasma.

DOI: [10.1103/PhysRevLett.109.205003](https://doi.org/10.1103/PhysRevLett.109.205003)

PACS numbers: 52.58.Lq, 52.59.Hq, 52.65.Rr

Introduction.—We describe here a new simulation capability: fully kinetic modeling of dense plasma focus (DPF) Z-pinch devices [1–4], including electrodes. This new model reproduces for the first time the neutron yields ($\sim 10^7$) and high-energy (MeV) beams observed experimentally in DPF devices. It exhibits plasma fluctuations near the lower hybrid frequency, consistent with the existence of the lower hybrid drift instability [5], long speculated to be a driver of anomalous resistivity [6] that creates such high gradients and produces energetic beams. It is the first self-consistent model of a DPF pinch that can be used hereafter as an exploratory tool to better understand the inner workings of one of the simplest and oldest plasma configurations.

A DPF Z pinch is a device consisting of two coaxially located electrodes with a high-voltage source at one end, typically a capacitor bank. In the presence of a low-pressure gas, the high-voltage source induces a plasma sheath formation at one end of the DPF. During the “run-down” phase, the plasma sheath is pushed down the length of the inner electrode through the $\mathbf{J} \times \mathbf{B}$ force, ionizing and sweeping up neutral gas as it accelerates. After the plasma sheath reaches the end of the inner electrode, it begins to collapse radially inward during the “run-in” phase. In the final “pinch” phase, the plasma implodes on axis, creating a high-density region that typically emits high-energy electron and ion beams, x rays, and (in the presence of D or D-T) neutrons (Fig. 1) [4].

Ion beams have been observed on a variety of DPFs [7–10] with energies up to 8 MeV in a cm-scale pinch region, implying gradients of order GV/m [8]. Several plausible mechanisms, both resistive and inductive, have been proposed to explain the increase in plasma impedance

that gives rise to these high gradients. However, previous experimental measurements and simulations have not definitively identified which of these mechanisms exist in DPF devices.

DPFs and other Z-pinch experiments have been modeled extensively using fluid codes [11–14]. Fluid simulations have been successful to some degree in predicting neutron yield on larger devices, where presumably thermonuclear fusion plays a sizeable role. However, on smaller devices where beam-target fusion dominates, fluid codes have not reproduced experimental neutron yields [11,13,15,16].

Previous work has also included a non-self-consistent test particle approach to look at kinetic effects [17–21], kinetic simulations of a Z-pinch device with scaled ion-electron mass [22], and kinetic simulations of a conventional gas-puff Z-pinch device [15,16]. In order to see kinetic effects in the final pinch phase of a DPF, such as beam formation and beam-target fusion, a self-consistent, fully kinetic approach is needed. The fully kinetic simulations shown here, which include the electrodes as well as

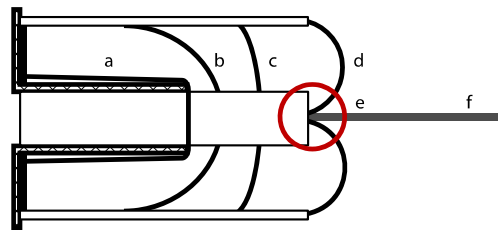


FIG. 1 (color online). Schematic of a dense plasma focus Z-pinch device, including flashover (a), run down (b and c), run in (d), pinch (e), and beam output (f).

the run-in phase, represent a significant improvement over the present day state of the art.

Simulation setup.—The fluid, hybrid, and fully kinetic calculations shown here were all performed in the particle-in-cell (PIC) code large scale plasmas (Lsp) [23]. Lsp uses an implicit algorithm to simultaneously calculate particle movements and electromagnetic fields, allowing for relatively long time steps and under-resolution of the plasma Debye length. The implicit algorithm is stable for $\omega_p \Delta t \gg 1$, provided that $\omega_c \Delta t < 0.5$, where ω_p and ω_c are the electron plasma and cyclotron frequencies and Δt is the simulation time step. Thus, the time step in the simulation, initially 2.5×10^{-4} ns, was decreased as the magnetic field increased, ending at 8.5×10^{-6} ns for the kinetic calculation.

The simulated electrode geometry is nominally matched to the existing DPF at Lawrence Livermore National Laboratory (LLNL), and dimensions are roughly within a factor of 2–4 of the majority of experimental DPFs built in the past 50 years [1]. A 5-cm-long anode (inner electrode) is represented by a conductive hollow tube with outer and inner radii of 1 and 0.5 cm, respectively. The cathode is represented by a conducting boundary at $r = 1.5$ cm.

The simulations are two dimensional (r, z) in cylindrical coordinates. The 151-by-322 grid in r and z , respectively, is overlaid on a 1.5 cm radius, 10 cm long cylinder.

The calculation is initialized at the end of the run-down phase (Fig. 2), with a 1-mm-width plasma sheath of uniform density. Initially, the sheath is traveling at a speed of $(B^2/2\mu_0\rho_0)^{1/2}$, where B is the magnetic field behind the sheath and ρ_0 is the neutral mass density in front of the sheath. This is the speed required to equalize the pressure on either side of the sheath. The neutral gas in the simulation begins with an atomic deuterium number density of 6.7×10^{16} cm $^{-3}$, corresponding to 1 torr of molecular deuterium at STP. The region behind the sheath is initially vacuum, because gas in that region would have been ionized and swept up during the run-down phase. The sheath is given an initial number density of 3.3×10^{17} cm $^{-3}$, assuming a 10% sweep efficiency of the neutral gas. In experiments with circular arrays of cathode rods instead of a solid cathode, some of the gas escapes between the rods.

The drive is modeled with a prescribed incoming voltage wave traveling the length of the anode, with a reflected

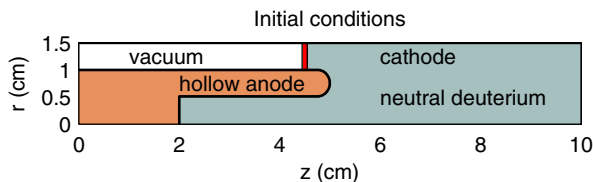


FIG. 2 (color online). Initial conditions for simulations. Plasma sheath (red) of both ions and electrons is centered at $z = 4.5$. The region behind the sheath is vacuum. In front of the sheath is neutral deuterium gas.

wave traveling back. At the beginning of the calculation, the incoming voltage wave is ramped up during the first 10 ns (before the run in), and then kept constant for the remainder of the simulation. The voltage drop across the electrodes is the difference between the incoming and reflected voltage waves, and is ~ 4 kV initially, when the plasma is very conductive. This results in a steady-state current (before the pinch) of 180 kA, consistent with the LLNL experiment.

Simulation results.—The ion number density at several time slices in the fully kinetic simulation is shown in Fig. 3, exhibiting the run-in and pinch phases of the DPF. Analogous two-fluid and hybrid (inertial fluid electrons, kinetic ions) simulations exhibit similar plasma sheath shape.

As the plasma runs in toward the axis, the impedance of the plasma increases, due to both resistive and inductive effects. This causes the current to dip and the voltage measured across the two electrodes to increase. The current, voltage, and plasma impedance are shown in Fig. 4 for the fluid, hybrid, and fully kinetic simulations. In the fully

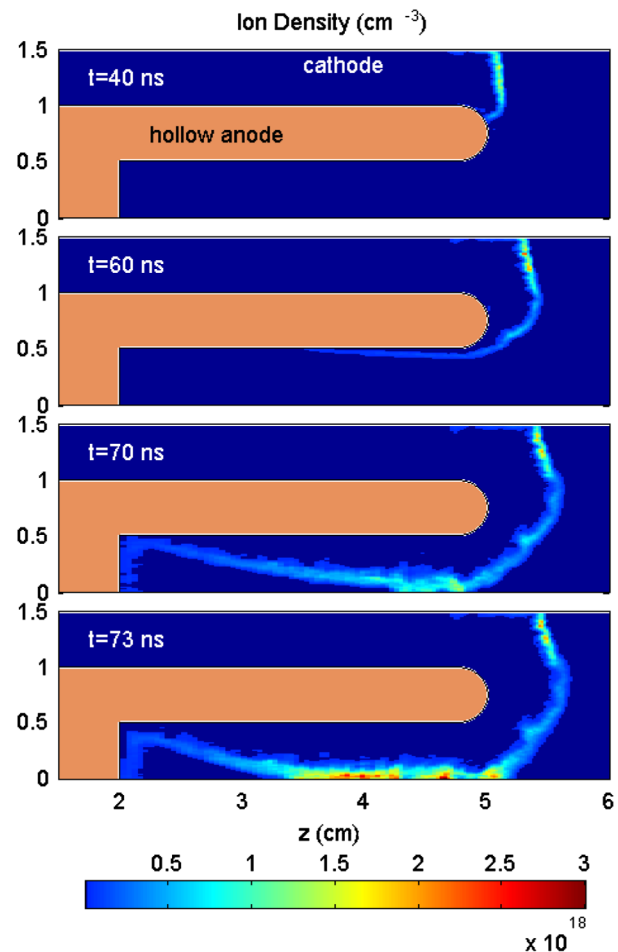


FIG. 3 (color online). Evolution of $D +$ number density during the run-in and pinch phases. The final frame shows the pinch, when the plasma reaches $r = 0$ and implodes.

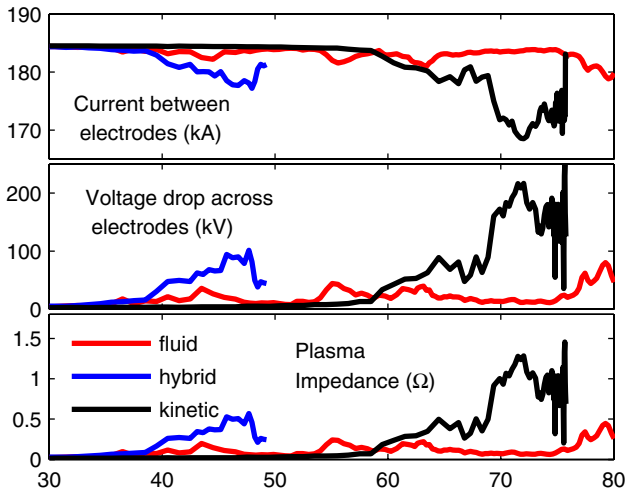


FIG. 4 (color online). Plasma current, voltage drop across electrodes, and plasma impedance for the fluid, hybrid, and kinetic simulations.

kinetic calculation, the current dips 15 kA, or 8%, during the pinch. This is consistent with current dips observed in the LLNL DPF experiment, which vary shot to shot, but that can be up to 40 kA when operating near 1 torr. The plasma impedance predicted in the fully kinetic case (20 m Ω at the beginning and 1 Ω during the pinch) is in line with measurements from DPFs in this energy class [1].

The z component of the electric field predicted by the fully kinetic simulation has quite a complex structure (Fig. 5). The E_z field is positive in some locations and negative in others, with the positive regions dominating and often higher in magnitude. This is consistent with the notion that a traditional DPF emits energetic ion beams in the forward direction and energetic electron beams in the reverse direction (when the anode is the inner electrode). Some experiments have reported a weak ion beam in the reverse direction as well [24]. This is consistent with the

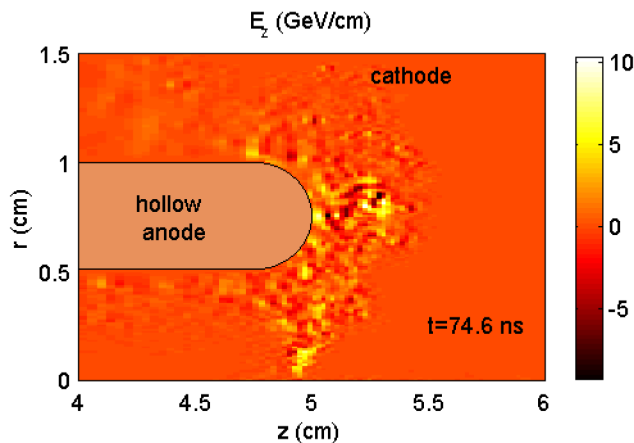


FIG. 5 (color online). The E_z field inside the fully kinetic simulation in the middle of the pinch, showing both positive and negative E_z fields. The pinch region is near $r = 0$ cm.

“pockets” of negative E_z fields predicted by the model. The fully kinetic model predicts ion and electron beams in both z directions, albeit with the much stronger beams in the forward direction.

Figure 6 shows the ion energy distribution inside the $z = 4$ to 6 cm region for the hybrid and fully kinetic simulations. The fully kinetic simulation predicts multiple MeV ions. While the energy distribution function inside the plasma cannot be directly compared with a beam energy measurement outside the plasma, the ion energies observed in the fully kinetic simulation are reasonably consistent with the experimentally measured ion beams. Ions of energies up to 8 MeV have been measured on kJ-class DPFs [8]. We have measured beams with energy in excess of 400 keV on the LLNL DPF, though higher-energy ions may exist below the noise limit of the beam diagnostic. No previous self-consistent DPF pinch simulation has predicted MeV-range ions. For the bulk plasma temperature, the kinetic simulation predicts ~ 12 keV ions and ~ 3 keV electrons in the hottest part of the pinch region.

The hybrid calculation, which exhibits a lower plasma impedance than the kinetic calculation (Fig. 4), does not predict ions of energies greater than ~ 200 keV. Presumably, this is because primarily inductive effects are driving the ion tail in the hybrid case, while both resistive and inductive effects create the ion tail in the fully kinetic case. Thus, fluid codes are not simply lacking in their ability to produce ion beams, as one might assume, but also in their ability to account for the kinetic effects that are postulated to be responsible for anomalous resistivity in pinch plasmas [6].

We recorded the local E_z field in the simulations at $r = 0.05$ cm, $z = 5$ cm every two time steps to look for high-frequency fluctuations that might indicate the presence of lower hybrid drift instability. The frequency

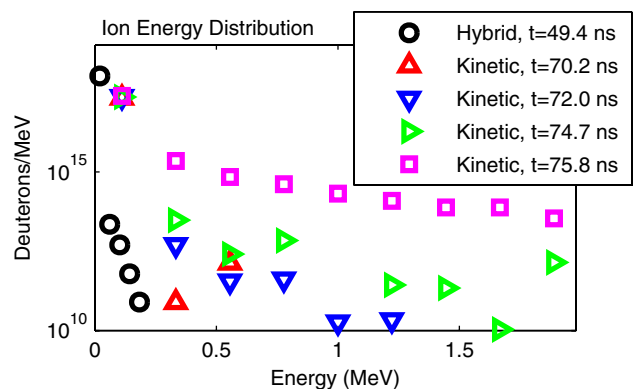


FIG. 6 (color online). Ion energy distribution for the hybrid simulation and for four time slices of the fully kinetic simulation. The hybrid simulation does not exhibit ions with energy greater than ~ 200 keV, and thus does not reproduce experimentally observed ion energies. The fully kinetic simulation exhibits the >1 MeV energy ions that have been observed on several DPF experiments [7–10].

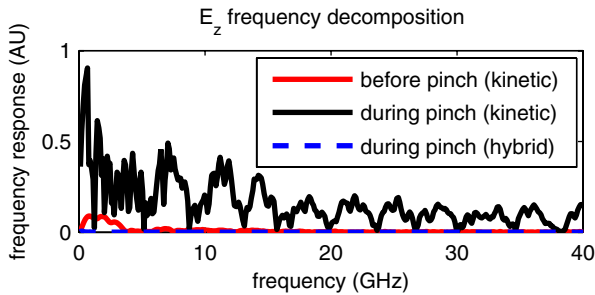


FIG. 7 (color online). Frequency decomposition of E_z field at $r = 0.05$ cm, $z = 5$ cm for a fully kinetic and hybrid simulation. A Fourier transform with rectangular window of width 10 ns is used. Just prior to the pinch (red), a frequency response at a few GHz appears in the kinetic simulation. During the pinch (black), a large frequency response appears at multiples of approximately 4 GHz. The lower hybrid frequency during the pinch phase ranges from 10 to 20 GHz, so these oscillations are in the range of those predicted analytically for the lower-hybrid-drift instability [5]. These oscillations are absent in the hybrid simulation (dashed blue).

decomposition in Fig. 7 reveals oscillations near the lower hybrid frequency during the pinch phase of the fully kinetic simulation, which are absent in the hybrid simulation. This is the first time oscillations of this frequency have been observed in a Z-pinch simulation.

Both thermonuclear and beam-target fusion can occur inside DPF plasmas. Lsp has a fusion module that creates fusion product particles based on the relative velocity between deuterium particles that collide (in the case of fluid deuterium, it uses the fluid temperature and density to calculate reaction rates). The total neutron production predicted in the fully kinetic calculation was 0.86×10^7 , consistent with our experimental DPF, which has a measured neutron yield of up to $\sim 2 \times 10^7$ at 180 kA. The hybrid simulation predicted 3.6×10^4 neutrons and the fluid simulation predicted no neutrons. Prior DPF and gas-puff Z-pinch fluid simulations have typically significantly underpredicted experimental neutron yield, particularly for low-current experiments such as ours. Presumably, this is because fluid simulations can only predict thermonuclear fusion, while lower-current experiments may be dominated by beam-target fusion [11,13,15,16].

Summary.—We have developed the first fully kinetic simulations of a DPF Z-pinch plasma, including electrodes and the run-in and pinch phases. These simulations predict for the first time both the high-energy ion beams and neutron yields that have been observed on numerous DPF experiments, results that cannot be reproduced in hybrid or fluid simulations. They also show plasma fluctuations near the lower hybrid frequency, suggesting that the lower hybrid drift instability may be present in the simulations.

The authors would like to thank Steve Falabella and Jennifer Ellsworth for their input and guidance on comparison with the experiment. We also thank David Rose for his assistance with the hybrid simulations. This work performed under the auspices of the U.S. Department of Energy by Lawrence Livermore National Laboratory under Contract No. DE-AC52-07NA27344 and supported by the Laboratory Directed Research and Development Program (11-ERD-063) at LLNL.

- [1] A. Bernard *et al.*, *J. Moscow Phys. Soc.* **8** (1998).
- [2] M. G. Haines, *Plasma Phys. Controlled Fusion* **53**, 093001 (2011).
- [3] J. W. Mather, *Phys. Fluids* **7**, S28 (1964).
- [4] J. W. Mather, *Phys. Fluids* **8**, 366 (1965).
- [5] N. A. Krall and P. C. Liewer, *Phys. Rev. A* **4**, 2094 (1971).
- [6] R. C. Davidson and N. T. Gladd, *Phys. Fluids* **18**, 1327 (1975).
- [7] L. Bertalot, H. Herold, U. Jäger, A. Mozer, T. Oppenländer, M. Sadowski, and H. Schmidt, *Phys. Lett.* **79A**, 389 (1980).
- [8] W. H. Bostick, H. Kilic, V. Nardi, and C. W. Powell, *Nucl. Fusion* **33**, 413 (1993).
- [9] W. Stygar, G. Gerdin, F. Venneri, and J. Mandrekas, *Nucl. Fusion* **22**, 1161 (1982).
- [10] R. L. Gullickson and H. L. Sahlin, *J. Appl. Phys.* **49**, 1099 (1978).
- [11] C. S. Kueny, D. G. Flicker, and D. V. Rose, Sandia National Laboratory Report No. SAND2009-6373, 2009.
- [12] S. Maxon and J. Eddleman, *Phys. Fluids* **21**, 1856 (1978).
- [13] D. E. Potter, *Phys. Fluids* **14**, 1911 (1971).
- [14] K. Behler and H. Bruhns, *Phys. Fluids* **30**, 3767 (1987).
- [15] D. R. Welch, D. V. Rose, R. E. Clark, C. B. Mostrom, W. A. Stygar, and R. J. Leeper, *Phys. Rev. Lett.* **103**, 25 (2009).
- [16] D. R. Welch, D. V. Rose, C. Thoma, R. E. Clark, C. B. Mostrom, W. A. Stygar, and R. J. Leeper, *Phys. Plasmas* **18**, 056303 (2011).
- [17] R. Deutsch and W. Kies, *Plasma Phys. Controlled Fusion* **30**, 263 (1988).
- [18] S. P. Gary and F. Hohl, *Phys. Fluids* **16**, 997 (1973).
- [19] M. G. Haines, *Nucl. Instrum. Methods Phys. Res.* **207**, 179 (1983).
- [20] Y. Kondoh and M. Mamada, *Phys. Fluids* **29**, 483 (1986).
- [21] V. Tang, M. L. Adams, and B. Rusnak, *IEEE Trans. Plasma Sci.* **38**, 719 (2010).
- [22] T. Haruki, H. R. Yousefi, K. Masugata, J.-I. Sakai, Y. Mizuguchi, N. Makino, and H. Ito, *Phys. Plasmas* **13**, 082106 (2006).
- [23] D. R. Welch, D. V. Rose, M. E. Cuneo, R. B. Campbell, and T. A. Mehlhorn, *Phys. Plasmas* **13**, 063105 (2006).
- [24] M. V. Roshan, P. Lee, S. Lee, A. Talebitaher, R. S. Rawat, and S. V. Springham, *Phys. Plasmas* **16**, 074506 (2009).